Eur. Radiol. 10, 1095–1100 (2000)

Abdominal radiology

European Radiology

Original article

Multifocal nodular fatty infiltration of the liver mimicking metastatic disease on CT: imaging findings and diagnosis using MR imaging

T. J. Kröncke[1], **M. Taupitz**[1], **D. Kivelitz**[1], **I. Scheer**[1], **U. Daberkow**[2], **B. Rudolph**[3], **B. Hamm**[1]

[1] Institut für Radiologie, Universitätsklinikum Charité, Humboldt-Universität zu Berlin, Schumannstraße 20–21, D-10117 Berlin, Germany
[2] IV Medizinische Klinik, Universitätsklinikum Charité, Humboldt-Universität zu Berlin, Schumannstraße 20–21, D-10117 Berlin, Germany
[3] Institut für Pathologie, Universitätsklinikum Charité, Humboldt-Universität zu Berlin, Schumannstraße 20–21, D-10117 Berlin, Germany

Received: 15 September 1999 Revised: 3 February 2000; Accepted: 7 February 2000

Abstract. The aim of this study was to describe the MR appearance of multifocal nodular fatty infiltration of the liver (MNFIL) using T1-weighted in-phase (IP) and opposed-phase (OP) gradient-echo as well as T2-weighted turbo-spin-echo sequences with fat suppression (FSTSE) and without (HASTE). Magnetic resonance imaging examinations at 1.5 T using T1-weighted IP and OP-GRE with fast low angle shot (FLASH) technique, and T2-weighted FSTSE, T2-weighted HASTE of 137 patients undergoing evaluation for focal liver lesions were reviewed. Five patients were identified in whom CT indicated metastatic disease; however, no liver malignancy was finally proven. Diagnosis was confirmed by biopsy ($n = 3$), additional wedge resection ($n = 1$) or follow-up MRI 6–12 months later ($n = 5$). Regarding the identified five patients, the number of focal liver lesions was 2 ($n = 2$) and more than 20 ($n = 3$). The MR imaging characteristics were as follows: OP-image: markedly hypointense ($n = 5$); IP image: isointense ($n = 2$) or slightly hyperintense ($n = 3$); T2-weighted FSTSE-image: isointense ($n = 5$); T2-weighted HASTE image isointense ($n = 1$); slightly hyperintense ($n = 4$). On OP images all lesions were sharply demarcated and of almost spherical configuration ($n = 5$). Further evaluation by histology or follow-up MR imaging did not give evidence of malignancy in any case. Histology revealed fatty infiltration of the liver parenchyma in three patients. Magnetic resonance follow-up showed complete resolution in two patients and no change in three patients. Multifocal nodular fatty infiltration can simulate metastatic disease on both CT and MR imaging. The combination of in-phase (IP) and opposed-phase (OP) gradient-echo imaging can reliably differentiate MNFIL from metastatic disease.

Correspondence to: T. J. Kröncke

Key words: MRI – Liver – Fatty infiltration – Opposed phase – Metastases

Introduction

Fatty infiltration of the liver (hepatic steatosis) in its diffuse and focal form is a well-recognized radiologic and histologic entity that has been observed in a variety of disorders including alcoholism, diabetes mellitus, obesity, tumor cachexia, congestive heart failure, and acquired porphyria cutanea tarda, as well as in patients receiving steroid medication or chemotherapy [1, 2, 3, 4]. Previous reports of fatty infiltration of the liver have emphasized its appearance on CT [3, 5, 6, 7, 8, 9]. Focal involvement poses diagnostic problems because the hypodense appearance on CT makes it difficult to differentiate fatty infiltration from metastatic disease, particularly when multiple lesions are present [4, 6, 7, 8, 9]. Biopsy or radionuclide scan used to be recommended in these cases. Reviewing 137 patients examined by MR imaging for focal liver lesions we found various types of fatty infiltration ranging from a diffuse form and circumscribed areas near anatomical landmarks to a distinct type characterized by multiple nodular areas not confined to any anatomical border. Herein we describe the appearance of this latter type of fatty infiltration – which we termed "multifocal nodular fatty infiltration of the liver" (MNFIL) – on various pulse sequences and a method to reliably differentiate it from malignancy.

Materials and methods

In 1997 and 1998, 137 patients underwent MR imaging for further evaluation of highly suspected malignant liver lesions on CT. All patients were examined prospectively according to the standardized protocol described

Fig. 1 a–f. Images of a 53-year-old patient with acquired porphyria tarda due to long-term exposure to hepatotoxic chemicals. On **a** unenhanced and **b** contrast material enhanced CT multiple hypodense non-enhancing lesions are present. Based on these findings, multiple metastases were suspected. **c** On T1-weighted gradient-recalled echo (GRE) opposed-phase and **d** T2-weighted half-Fourier acquired single-shot turbo spin echo (HASTE) images these lesions appear hypo- and hyperintense, respectively. However, on **e** T1-weighted GRE in-phase images lesions appear hyperintense, and on **f** fat-suppressed T2-weighted turbo spin-echo (FSTSE) images lesions are not visible, indicating the presence of multifocal nodular fatty infiltration of the liver (MNFIL)

herein. In five of these patients with multiple liver lesions present on CT and MR imaging, malignancy was finally ruled out by histology or follow-up. Underlying diseases in four of these five patients were ovarian neoplasm ($n = 1$), breast cancer ($n = 1$), gastric cancer combined with marked obesity ($n = 1$), and acquired porphyria tarda ($n = 1$) due to long-term exposure to hepatotoxic chemicals. In one patient no underlying disease process could be identified. Diagnoses were confirmed by histology and follow-up MR imaging ($n = 3$) or follow-up MR imaging alone ($n = 2$). Two patients had repeated biopsies. In one patient wedge resection was performed in addition to previous biopsy. The interval of follow-up MR imaging ranged from 6 to 12 months. Magnetic resonance imaging was performed with a 1.5 T whole-body superconducting system (Magnetom Vision, Siemens, Erlangen, Germany) using a four-element body phased-array coil. The imaging protocol included transaxial images with 7-mm slice thickness and an intersection gap of 1.4 mm for T1-weighted gradient-echo (GRE) in-phase (IP; TR = 175 ms, TE = 5.3 ms, flip angle = 90 °) and opposed-phase (OP) images (TR = 175 ms, TE = 2.77 ms, flip angle = 90 °) using two different echoes of the same pulse sequence, transaxial T2-weighted fat-suppressed turbo spin-echo (FSTSE; TR = 5000 ms, TE = 80 ms) and transaxial half-Fourier single-shot turbo spin-echo images (HASTE; TR = ∞/TE = 64 ms) with 8-mm slice thickness covering the whole liver. The GRE and HASTE images were obtained during a single end-inspiratory breath-hold of 21 s. In addition, a dynamic gadolinium-enhanced (gadopentetate dimeglumine, Magnevist, Schering, Berlin, Germany) study was performed using an in-phase GRE sequence.

Results

Based on CT, malignancy was suspected in all five cases because of multiple hypodense liver lesions of almost spherical configuration (Fig. 1 a). These lesions ranged in diameter from less than 5 mm to 2 cm, appeared partially confluent, and had attenuation values of approximately 30 HU. Scans obtained in the arterial phase (AP) and the portal venous phase (PVP) after application of contrast material showed no enhancement of the lesions during either phase (Fig. 1 b). Magnetic resonance imaging identified more than 20 lesions in three patients (Figs. 1, 2) and two lesions in two patients (Fig. 3) with lesion diameters previously described for CT. The lesions were not confined to any anatomical landmark, and no relationship was found between their diameters and their distribution in the liver. There was no obvious mass effect of the lesions observable. All lesions were sharply demarcated and of almost spherical configuration on OP images ($n = 5$). All lesions showed a substantial change in signal intensity (SI) from isointense ($n = 2$; Fig. 2 c) or slightly hyperintense ($n = 3$; Figs. 1 e, 3 c) on IP images to markedly hypointense on OP images ($n = 5$; Figs. 1 c, 2 a, 3 a) compared with surrounding liver parenchyma which showed no evident change in SI from normal. On T2-weighted HASTE images the lesions were isointense ($n = 1$) or slightly hyperintense ($n = 4$; Figs. 1 d, 2 b, 3 b). On T2-weighted FSTSE images the lesions could not be identified (Fig. 1 f) since they were isointense to the normal liver parenchyma ($n = 5$).

Histologic correlation was available in three patients. Histology of a wedge resection specimen in one case and biopsy in two patients showed slight fibrosis, siderosis, and intracellular fat deposition in up to 30 % of the liver parenchyma and yielded no malignant cells. Follow-up MR imaging was performed in all five patients and revealed complete resolution of the lesions in two patients. In one of them resolution was attributable to gastrectomy performed during the follow-up interval and subsequent substantial weight reduction by over 40 % of previous body weight (Fig. 2d–f). In three patients no change in the MR imaging appearance of the lesions was noted compared with the previous examination.

Discussion

Hepatic steatosis is a functional disorder of the liver resulting from metabolic changes. Although diffuse and focal fatty transformation of the liver parenchyma has been observed in a heterogeneous group of diseases, the underlying pathophysiologic mechanism is thought to be either tissue hypoxia, increased portal flow, or delivery of unknown toxic substances from the portal vein [1, 2, 11] with subsequent accumulation of intracellular triglycerides in the form of fat droplets. Diminished perfusion was postulated as the main cause for hypoxia since larger areas of focal fatty infiltration were found subcapsular at the periphery of the portal venous and arterial circulation [1]. The majority of patients with pure hepatic steatosis and no signs of coexisting hepatitis or fibrosis are considered to have a benign condition which may resolve quickly once the underlying pathology subsides. Regarding the different patterns of fatty infiltration of the liver, no established terminology exists. The various types of fatty infiltration can be divided into two main groups: diffuse and focal fatty infiltration. Diffuse fatty change of the liver involves the entire organ and shows reduced attenuation values on CT. The CT findings together with the clinical history are usually diagnostic for diffuse fatty infiltration.

Generally, the focal type is easily identified on CT as a nonspherical, poorly marginated low-density area which is arranged in a geographic pattern and lacks a significant mass effect. Laparoscopy and macroscopic pathology show areas of focal fatty infiltration consisting of yellow-white nodules that have a scalloped border, contain otherwise normal hepatocytes with cytoplasmic vacuoles of lipid, and are histologically surrounded by liver parenchyma with little or no fatty change [1, 11]. Focal fatty infiltration has been found predominantly near the medial segment of the left lobe of the liver adjacent to the falciform ligament and the gallbladder bed [12, 13] and has been attributed to vascular variants in the venous blood supply of the liver [14, 15, 16].

Occasionally, fatty infiltration of the liver presents with multiple, usually more than 20, nodular lesions of various diameters scattered throughout the liver. The lesions may be confluent and follow no anatomical structure. Multifocal nodular fatty infiltration of the liver (MNFIL), as described in the present paper, has not yet been recognized as a specific type of fatty infiltration in the literature, although its appearance has been reported in a few cases on CT [4, 5, 6, 7, 8, 9] and on MR imag-

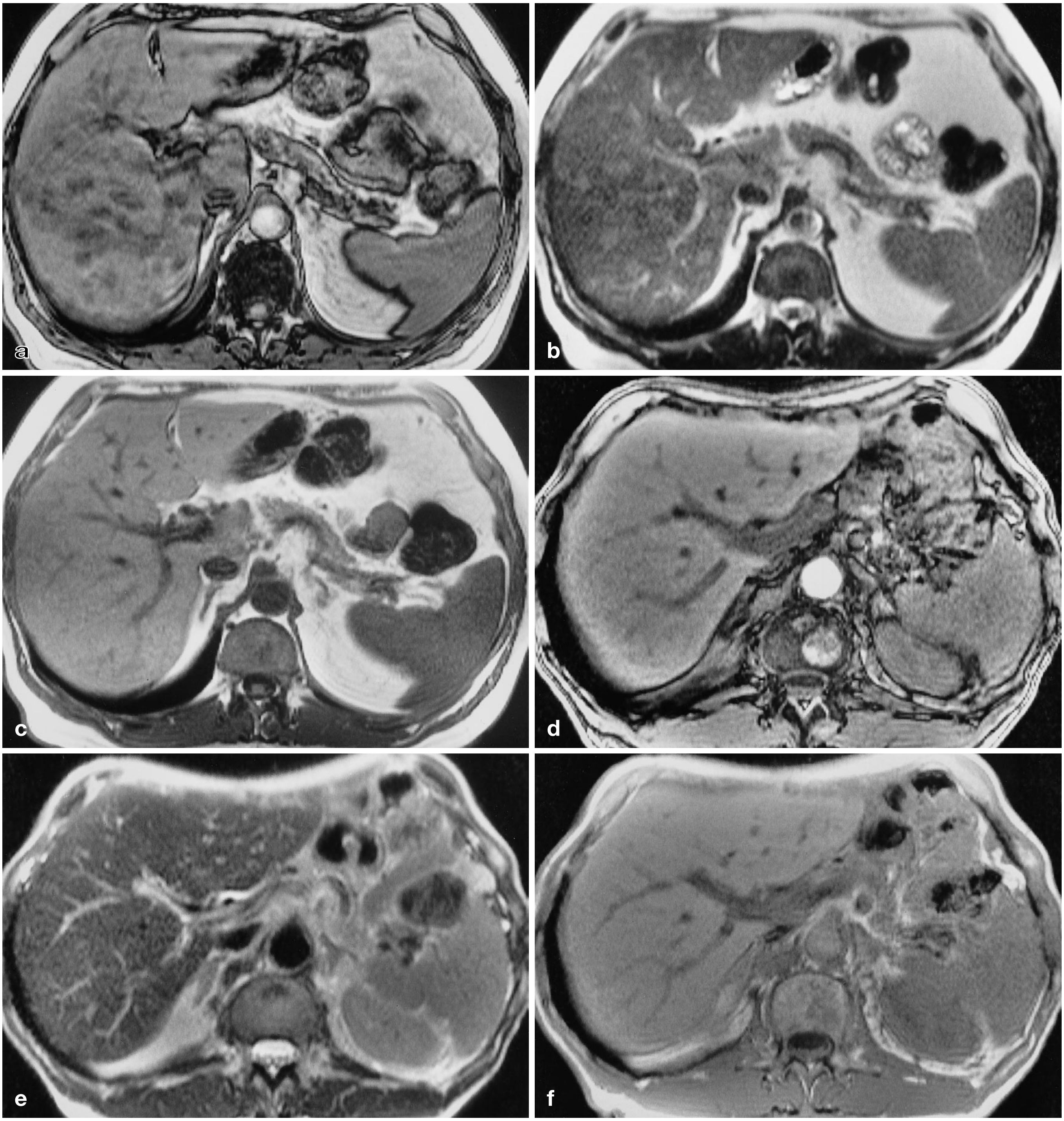

Fig. 2 a–f. Magnetic resonance images of a 59-year-old patient with gastric cancer (not shown) and marked obesity. **a** On T1-weighted GRE opposed-phase images multiple nodular hypointense lesions are present. **b** On T2-weighted HASTE images the lesions are hyperintense. **c** T1-weighted GRE in-phase images do not show any lesion. Follow-up MR imaging was performed after gastrectomy and a 1-year interval between both exams. A marked reduction in body weight is seen by comparing the thickness of the subcutaneous fat layer on both exams. **d** On T1-weighted GRE opposed-phase and on **e** T2-weighted HASTE images, as well as **f** T1-weighted GRE in-phase images, no lesions are detectable, demonstrating resolution of benign MNFIL

ing [10, 17, 18]. Generic imaging clues have been reported for focal fatty infiltration of the liver such as lack of a mass effect, undistorted vessels traversing the area of interest [2, 5], and a central core of hepatic tissue appearing normal within an area of fatty change [8], but they are obviously of limited value in cases of MNFIL as demonstrated in the present study.

A comprehensive description of the MR imaging features of MNFIL has not yet been given. Only subsets of imaging sequences have been employed by different researchers. Itai et al. [18] and Dao et al. [17] described the appearance of MNFIL on T1-weighted spin-echo se-

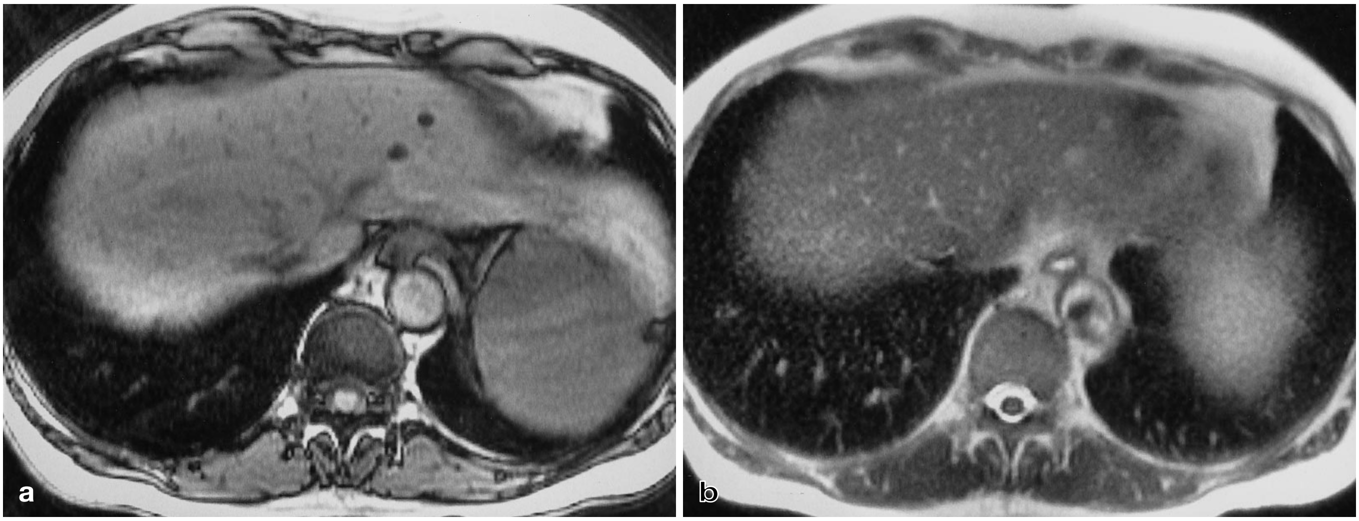

Fig. 3 a–c. Magnetic resonance images of a 77-year-old patient with breast cancer and suspected liver metastases on CT (not shown). **a** On T1-weighted GRE opposed-phase images two sharply demarcated focal liver lesions are seen in the left lobe of the liver, which show homogeneously low signal intensity compared with surrounding liver parenchyma. **b** On T2-weighted HASTE images and on **c** T1-weighted GRE in-phase images the two lesions are slightly hyperintense. Comparison of T1-weighted GRE in-phase and opposed-phase images confirms the diagnosis of MNFIL and rules out malignancy

quences, and Mitchell [10] demonstrated its appearance on a GRE OP sequence and SE sequences in one case. Magnetic resonance imaging using conventional spin-echo pulse sequences can detect areas of fatty infiltration as hyperintense lesions on T1- and T2-weighted images if fat content is high enough to alter signal intensity [17, 18,19]. In experimental models the increase in signal intensity on conventional T1- and T2-weighted SE images is slight, despite a massive increase in triglyceride content of hepatocytes [19].

In the present study the MR appearance of MNFIL has been evaluated using a broad spectrum of imaging sequences. In our study the fatty infiltrations were seen as slightly hyperintense almost spherical lesions in three patients and not detectable in two patients by means of GRE IP imaging. With the single-shot turbo spin-echo technique (HASTE) MNFIL was detected in four of the five patients. Since metastases as well as MNFIL appear bright on T2-weighted HASTE images, the diagnosis of MNFIL cannot be made confidently using HASTE images. Spectral fat suppression may be helpful in the diagnosis of MNFIL, since it allows selective suppression of areas of fat; however, this method is unsatisfactory because diagnosis relies on not seeing a (suppressed) lesion rather than positively diagnosing its presence.

By far, the most sensitive MR method to detect intracellular fat deposition in hepatocytes is the use of an OP gradient-echo pulse sequence as shown in the present and previous studies [2, 10, 20, 21, 22]. The GRE OP imaging technique uses the destructive interference of opposing SI from lipid and water protons, most prominent in a voxel containing neither pure fat nor pure water, which is the case in MNFIL. In all five cases presented in this study it was possible to identify lesions with increased intracellular fat as sharply demarcated, almost spherical nodules of low signal intensity on OP images compared with IP images.

Regarding the trend toward fast imaging techniques using powerful gradient systems that allow GRE imaging with a TE of less than 4–5 ms, it is essential to be aware of possible pitfalls when using T1-weighted GRE imaging or T2-weighted TSE sequences. At currently employed field strengths of 0.5–1.5 T unexpected opposed-phase imaging conditions can be encountered when T1-weighted GRE imaging is used. This can be misleading in the diagnosis of MNFIL since fatty lesions may be misinterpreted as metastatic disease due to their hypointense appearance on T1-weighted GRE OP images. Therefore, we recommend to use a combination of GRE IP- and OP images in cases where MNFIL is suspected. Alternatively, fat-suppressed T2-weighted TSE sequences can be used to exclude malignancy.

Conclusion

Multifocal nodular fatty infiltration of the liver is a rare benign entity with a favorable outcome that should be considered as a cause for multiple hypodense lesions on CT. Relying on TSE sequences or GRE OP images alone, MNFIL may be confused with malignancy on MR imaging. A thorough evaluation of the liver should therefore include a combination of GRE OP- and IP sequences, which can reliably differentiate MNFIL from metastases. Alternatively, a fat-suppressed T2-weighted TSE sequence is recommended as part of the imaging protocol.

Acknowledgement. We thank B. Herwig for assistance translating the manuscript.

References

1. Brawer MK, Garth EA, Lewin KJ (1980) Focal fatty infiltration of the liver, a hitherto poorly recognized entity. Gastroenterology 78: 247–252
2. Siegelman ES (1997) MR-imaging of diffuse liver disease: hepatic fat and iron. Magn Reson Imaging Clin North Am 5: 347–365
3. El-Hassan YA, Ezzeldin MI, Al-Mulhim FA, Nabhan AA, Chammas MY (1992) Fatty infiltration of the liver: analysis of prevalence, radiological and clinical features and influence on patient management. Br J Radiol 65: 774–778
4. Flueckinger F, Steiner H, Leitinger Hoedl S, Deu E (1991) Nodular focal fatty infiltration of the liver in acquired porphyria cutanea tarda. Gastrointest Radiol 16: 237–239
5. Halvorsen RA, Korobkin M, Ram PC, Thompson WM (1982) CT appearance of focal fatty infiltration of the liver. AJR 139: 277–281
6. Baker ME, Silverman PM (1985) Nodular focal fatty infiltration of the liver: CT appearance. AJR 145: 79–80
7. Yates CK, Streight RA (1986) Focal fatty infiltration of the liver simulating metastatic disease. Radiology 159: 83–84
8. Flournoy JG, Potter JL, Sullivan BM, Gerza CB, Ramzy I (1984) CT appearance of multifocal hepatic steatosis. J Comput Assist Tomogr 8: 1192–1194
9. Gaa J (1993) An unusual case of multifocal annular fatty liver. Fortschr Röntgenstr 158: 76–77
10. Mitchell DG (1992) Focal manifestations of diffuse liver disease at MR imaging. Radiology 185: 1–11
11. Layfield LJ (1994) Focal fatty change of the liver: cytologic findings in a radiographic mimic of metastases. Diagn Cytopathol 11: 385–389
12. Yoshikawa J, Matsui O, Takashima T, Sugiura H, Katayama K, Nishida Y, Tsuji M (1987) Focal fatty change of the liver adjacent to the falciform ligament: CT and sonographic findings in five surgically confirmed cases. AJR 149: 491–494
13. Soyer P, Devine N, Somveille E et al. (1996) Hepatic pseudolesion around the falcifom ligament: prevalence on CT examination. Abdom Imaging 21: 324–328
14. Paulson RK, Baker ME, Sprizer CE et al. (1993) Focal fatty infiltration: a cause of nontumorous defects in the left hepatic lobe during CT arterial portography. J Comput Assist Tomogr 17: 590–595
15. Kawamori Y, Matsui O, Takahashi S, Kadoya M, Takashima T, Miyayama S (1996) Focal hepatic fatty infiltration in the posterior edge of the medial segment associated with aberrant gastric drainage: CT, US and MR findings. J Comput Assist Tomogr 20: 356–359
16. Itai Y, Matsui O (1999) "Nonportal" splanchnic venous supply to the liver: abnormal findings on CT, US and MRI. Eur Radiol 9: 237–243
17. Dao TH, Mathieu D, Nguyen-tan T, Derhy S, Vasile N (1991) Value of MR-imaging in evaluating focal fatty infiltration of the liver: preliminary study. Radiographics 11: 1003–1012
18. Itai Y, Kurosaki Y, Teraoka T (1993) Micronodular focal fatty infiltration of the liver. Fortschr Röntgenstr 159: 402–404
19. Stark DD, Bass NM, Moss AA et al. (1983) Nuclear magnetic resonance imaging of experimental induced liver disease. Radiology 148: 743–751
20. Wehrli FW, Perkins TG, Shimakawa A, Roberts F (1987) Chemical shift induced amplitude modulations in images obtained with gradient refocusing. Magn Reson Imaging 5: 157–158
21. Mitchell DG, Kim I, Chang TS et al. (1991) Fatty liver. Chemical shift phase difference and suppression magnetic resonance imaging techniques in animals, phantoms, and humans. Invest Radiol 26: 1041–1052
22. Levenson H, Greensite F, Hoefs J et al. (1991) Fatty infiltration of the liver: quantification with phase-contrast MR imaging at 1.5 T vs Biopsy. AJR 156: 307–312